

Expression of CD91 in extracellular vesicles: A potential biomarker for the diagnosis of non-small cell lung cancer

Shayista Akbar, Shahnaz Qadri, Sarmadia Ashraf, Aijaz Parray, Afsheen Raza, Wafa Abualainin, Said Dermime, Yousef Haik

Item type

Journal Contribution

Terms of use

This work is licensed under a [CC BY 4.0](https://creativecommons.org/licenses/by/4.0/) license

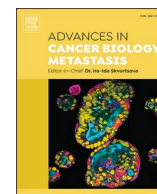
This version is available at

https://manara.qnl.qa/articles/journal_contribution/Expression_of_CD91_in_extracellular_vesicles_A_potential_biomarker_for_the_small_cell_lung_cancer/26947009/1

Access the item on Manara for more information about usage details and recommended citation.

Posted on Manara – Qatar Research Repository on

2022-05-26



Expression of CD91 in extracellular vesicles: A potential biomarker for the diagnosis of non-small cell lung cancer

Shayista Akbar^a, Shahnaz Qadri^{b,h,*}, Sarmadia Ashraf^a, Aijaz Parray^d, Afsheen Raza^e, Wafa Abualainin^f, Said Dermime^e, Yousef Haik^{c,g,**}

^a College of Health and Life Science, Hamad Bin Khalifa University, Qatar

^b College of Science and Engineering, Hamad Bin Khalifa University, Qatar

^c College of Engineering, Texas A&M University Kingsville, Texas, USA

^d Neuroscience Institute, Hamad Medical Corporation, Doha, Qatar

^e Translational Cancer Research Facility, National Center for Cancer Care and Research, Hamad Medical Corporation, Doha, Qatar

^f Diagnostic Genomic Division, Solid Tumor Section, Department of Laboratory Medicine and Pathology, Hamad Medical Corporation, Doha, Qatar

^g Brigham Women Hospital, Harvard University, 221 Longwood Ave, Boston, MA, 02115, USA

^h Irma Lerma Rangel College of Pharmacy, Texas A&M University, USA

ARTICLE INFO

Keywords:

Extracellular vesicles

Exosomes

Microparticles

Microvesicles

CD91

Low density lipoprotein receptor-related protein 1 (LRP1)

Non-small cell lung cancer

ABSTRACT

Lung cancer is the leading cause of death; by the time it is diagnosed, the patient is usually in late-stage grade IV. Late-stage lung cancer is mainly associated with metastasis in the liver, brain, and lymphoid tissues; as a result, a localized lung cancer treatment remains meaningless. Early diagnosis of non-small cell lung cancer (NSCLC) may be curable or will improve the survival rate. Although with advanced developments to screen high-risk patients by LDCT scan, false-positive rates and limited resolution necessitated the development of advanced diagnostic techniques for NSCLC. Extracellular vesicles (EVs) released from cells freely circulate in the blood and contain various transmembrane proteins, and they may be a non-invasive biomarker for cancer diagnosis and prognosis. Current studies predict that the CD91 marker in EVs may be a potential biomarker of NSCLC; however, the expression of CD91 in lung cancer tissues is not fully known. Here, this study determines the differential expression of CD91 in lung cancer cells and in circulating EVs in blood as a potential biomarker of NSCLC patients. Our results confirmed the expression of CD91 in NCI-H1975 cultured cells and NSCLC lung biopsy tissues. Furthermore, biophysical characterization of EVs from lung cancer cells determines the substantial expression of CD91, which the Transmission Electron Microscope confirms. Thus, this study suggests EVs containing CD91 could be an asset to studying the development of diagnostic and prognostic biomarkers in NSCLC disease.

1. Introduction

Lung cancer is the world's second most common cancer and the leading cause of cancer-related mortality, with 2.21 million new cases and nearly 1.80 million deaths in 2020 [1]. There are two distinct types of lung cancer: Non-small cell lung cancer (NSCLC) and small cell lung cancer (SCLC). NSCLC is the most prevalent form of lung cancer, accounting for up to 85% of all cases [2,3], with adenocarcinoma (ADC) and squamous cell carcinoma (SqCC) being the second most common subtypes of NSCLC [3]. Early diagnosis and treatment of NSCLC improve the 5-year survival rate to 75–90% [4]. The gold standard for clinical diagnosis is computed tomography (CT) scan, which is limited due to

tumor to background ratio and tumor sizes of less than 1 cm. More recently, the national lung screening trial (NLST) and NELSON used low-dose CT (LDCT) as a main strategy for early detection with substantial reduction in lung cancer mortality in the high-risk populations [5–8]. Despite the effectiveness of low-dose helical CT in early diagnosis of NSCLC in high-risk patients (e.g., heavy smokers), the NLST reported a substantially high false-positive rate from the benign tumors [9,10]. Clinically, tumors detected by CT scans need to be confirmed by tissue biopsies. At present, there are no blood-based clinically approved biomarkers for the lung cancer diagnosis and prognosis which could help to reduce the mortality rate and provide noninvasive and less expensive method for disease prognosis. Therefore, novel, and reliable biomarker

* Corresponding author. Irma Lerma Rangel College of Pharmacy, Texas A&M University, USA.

** Corresponding author. Department of Mechanical and Industrial Engineering, Texas A&M University Kingsville, USA.

E-mail addresses: shahnaz.qadri@tamuk.edu (S. Qadri), yousef.haik@tamuk.edu (Y. Haik).

<https://doi.org/10.1016/j.adcanc.2022.100046>

Received 14 November 2021; Received in revised form 13 May 2022; Accepted 19 May 2022

Available online 22 May 2022

2667-3940/© 2022 The Authors. Published by Elsevier B.V. This is an open access article under the CC BY license (<http://creativecommons.org/licenses/by/4.0/>).

for early detection of NSCLC diagnostic strategies with the potential to reduce mortality are urgently needed.

Recent studies report extracellular vesicles (EVs) as useful diagnostic, predictive and prognostic biomarkers in several cancers, including lung cancer [11].

EVs are cell-derived nano-sized membrane-bound vesicles released by almost all cell types and are found in nearly all bodily fluids [12]. EVs play a critical role as signaling vehicles to mediate intercellular communication and have therefore emerged as promising tools for studying and treating diseases, including lung cancer [13]. Based on their biogenesis, EVs are broadly classified into three groups: (1) small vesicles (40–200 nm), also referred to as exosomes, (2) large microvesicle (200–1000 nm) derived from the plasma membrane, (3) and larger apoptotic bodies (>1 µm) [14]. The lipids and proteins from the plasma membrane are retained by these vesicles, which directly bud off by fission in the cell's extracellular space as microvesicles [12]. Exosomes are typically considered endosomal origin and are secreted by most cell types through a well-defined intracellular route [15,16]. These small vesicles carry a full range of biomolecule cargo, such as DNA, RNA, miRNAs, proteins, cytokines, and chemokines from their originating cells [17,18]. Therefore, exosomes possess a high biomarker potential, mainly because they are easily accessible from body fluids and capable of representing their parental cells [19]. In addition, exosomes contain a cholesterol-rich lipid bilayer membrane, and they can protect their cargo from enzymatic degradation by extracellular proteases in biofluids and are highly stable in storage conditions [20,21]. Further, an appealing feature of the exosomes-based biomarkers is the significant reduction in the sample complexity compared to the whole blood [22]. The low-density lipoprotein receptor-related protein 1 (LRP1 or CD91) has been reported as upregulated in NSCLC patients [23], and studies have also identified CD91 in extracellular vesicles with the diagnostic potential for lung cancer [24]. CD91 is a type-1 transmembrane receptor that mediates ligand endocytosis and cargo trafficking to lysosomes [25]. CD91 is also reported as a signaling receptor regulating cytokine secretion, phagocytosis, and migration of cells in the immune system [26,27]. Besides the expression of CD91 in immune cells, the fibroblasts, neurons, and hepatocytes also express CD91; however, its function is not known [28]. The function of CD91 in immune cells involves immunosurveillance and stimulation of cytokines to initiate antitumor response [29,30]. Nonetheless, the role of CD91 in other types of cells is not clearly understood thus, it is evident that CD91 in serum or plasma derived EVs are released from diverse types of tissues and cells.

The proteomics analysis of plasma-derived exosomes in NSCLC patients identified 5-fold higher expression of CD91 when compared to healthy controls [31]. But the expression of CD91 in lung cancer cells has not been fully validated. However, it was reported that CD91 might not be expressed in lung cancer cells; instead, expressed in stromal cells surrounding lung tissues [32]. Therefore, to determine CD91 as a potential biomarker of NSCLC, it is imperative to validate the expression of CD91 in lung cancer cells and in EVs derived from lung cancer cells.

Click or tap here to enter text. Click or tap here to enter text. Click or tap here to enter text. Click or tap here to enter text. Hence, this study will characterize and confirm the expression of CD91 in lung cancer tissues and characterize CD91 positive EVs derived from lung cancer cells to validate the possibility of CD91 as a potential biomarker in NSCLC patients.

2. Materials and methods

2.1. Cell culture

The cell lines MCF-10A (immortalized, non-malignant human mammary cell line), MCF-7 (human breast cancer cell line), NCI-H1975 (human NSCLC cell line) and LL-24 (normal lung cell line) used in this study were purchased from ATCC. MCF-10A, MCF-7 and LL-24 were cultured in complete Dulbecco's minimal essential medium (DMEM;

Gibco#41966–029) high glucose (4.5 g/L) containing 10% fetal bovine serum (FBS; Gibco#10082–147), 1% penicillin and streptomycin at 37 °C and 5% CO₂. The NCI-H1975, an NSCLC cell line was cultured in RPMI-1640 medium (Cat. # 21875–034 Gibco) supplemented with 10% FBS, 1% penicillin and streptomycin at 37 °C and 5% CO₂.

2.2. CD91 immunofluorescence imaging

The cells MCF-10A, MCF-7, NCI-H1975 and LL-24 were seeded in 35mm × 10 mm tissue culture treated imaging dishes (cat. # 0030740.009 Eppendorf) in triplicates. At 80% confluency, the cells were washed with 1X PBS and fixed with 4% Formaldehyde (cat. #F8775 Sigma Aldrich) in 1X PBS for 8 min and then incubated in blocking buffer consisting of 4% BSA, 0.3 M glycine in 0.1% PBS-Tween (cat. # 28321 Thermo Scientific) for 1 h to permeabilize the cells and prevent non-specific protein binding. The cells were then incubated with the antibody (#ab20384, Abcam) at a dilution of 1:800 overnight at 4 °C. The secondary antibody Alexa Fluor® 488 goat anti-mouse IgG (H + L) (ab150113, Abcam) was used at a 1/1000 dilution for 1 h. DAPI (Cat. # 62248, Thermo Scientific) was used to stain the cell nuclei at a concentration of 1 µl/ml, and Alexa Fluor® 594-WGA (wheat germ agglutinin, cat. # 790162 MP. Biomedicals) was used to label plasma membranes. Fluorescent imaging was performed using Olympus IX73 manual inverted Fluorescence microscope. The 16 channel PE-4000 Cool LED light connected with microscope through optic fiber was used for excitation of fluorophores. Images were taken using 60x objective (U Plan SAPO 60x/1.35 oil) by Zyla 4.2 Andor sCMOS camera with 6.5 × 6.5 µm pixel size and maximum active pixels 2048 × 2048. Image processing was done by NIH image J software.

2.3. Isolation of EVs from cell culture

Cells were grown to 80% confluency, washed 2 times with PBS and serum free media was added and incubated at 37 °C in 5% CO₂ incubator. The medium was harvested after 48 h and centrifuged at 400×g for 7 min at 4 °C to remove cells and cellular debris. The supernatant was again centrifuged at 5000×g for 30 min to remove the large microparticles. The supernatant was concentrated to 2 ml using 100K concentrator (Thermo Fisher Scientific #88533) and transferred to 2 ml tube and centrifuged at 20,000×g for 30 min to isolate microparticles. Further, cell culture medium was subjected to ultracentrifugation (Hitachi CP100NX) at 100,000×g for 2 h at 4 °C to isolate the exosomes. Ultracentrifugation was repeated twice to minimize contamination of the soluble proteins. Subsequently, the exosomes were resuspended in 50 mL of PBS and were stored in 10 mL aliquots in different microcentrifuge tubes, stored at –20 °C until further use.

2.4. Patient recruitment and plasma preparation

The study was approved by the local Institutional Review Board and Human Research Ethics committee of the Hamad Medical Corporation (HMC), Qatar under IRB number: (# HMC, IRB, MRC 01-20-507). All subjects donating blood specimens for this study signed an informed consent in accordance with the Declaration of Helsinki. A total of 5 potentially eligible NSCLC patients having EGFR positive/negative mutations were recruited from National Centre for Cancer Care and Research (NCCCR), HMC, Qatar. Four healthy volunteers without lung cancer or any other disease were also included in this study. Whole blood was collected in vacutainer tubes and centrifuged at 1000×g for 10 min to collect the plasma. The plasma was aliquoted and stored at –20 °C until further experimental work.

Tumor biopsy formalin fixed paraffin embedded (FFPE) tissue sections of five NSCLC patients are obtained from Department of Laboratory Medicine and Pathology, Hamad Medical corporation, and are used for CD91 immunohistochemistry study. Prior to immunohistochemistry, these samples are tested for EGFR hotspot analysis following DNA

extraction from Formalin (FFPE), all procedures are performed at Pathology lab, Hamad Medical Corporation.

2.5. Isolation of EVs from plasma

The 500 mL of frozen plasma samples were thawed and diluted with PBS buffer (1:3) to decrease the viscosity. Protease inhibitors cocktail (Thermo fisher scientific, #78425) was added to the diluted samples, and centrifuged at 4500×g for 10 min at 4 °C to remove the cell debris. Furthermore, supernatant was collected and centrifuged at 20,000×g for 30 min at 4 °C to isolate the microparticles (MPs). Clarified supernatant was then centrifuged in Hitachi CP100NX ultracentrifuge at 100,000×g at 4 °C for 2 h with swing bucket rotor (P55ST2) to pellet exosomes. A second round of ultracentrifugation was carried out to improve the purity of exosomes obtained and the resulting exosome pellets were resuspended in PBS according to initial volumes and stored at −20 °C until further experiment.

2.6. Biotinylation of CD91, preparation of magnetic beads and immunocapture bead assay

The capturing antibody CD91 (ab 20384; Abcam) was biotinylated by adding 10 µl of 100 mM EZ-Link NHS-PEG4-Biotin (# A39259, Thermo fisher scientific) and 300 µl of 50 mM Borate buffer (pH 8.4) to each antibody and incubated for 2 h at 4 °C with continuous mixing on rotor device. After 2 h of incubation, 100 µl of 0.1 M Glycine was added and incubated again for 30 min at 4 °C with continuous mixing to quench the active biotin esters. The biotinylated antibodies were filtered using 10KD nanosep (#OD010C34, Pall Life Science) and further washed 8 times using the same centrifugal device. The biotinylated antibodies were resuspended in the same initial volume and stored at the same condition that was optimal for the non-biotinylated antibodies.

100 µg of magnetic beads coated with streptavidin (Dynabeads MyOne Streptavidin C1, Invitrogen, #65001) was suspended in 500 µl of 0.1% PBST and washed using magnetic separation. The beads were placed on magnetic rack for 3–5 min and the supernatant was discarded. The washing was repeated 4 times, two in 0.1%PBST and two washes in PBS. After last wash, the beads were resuspended in 200 µl PBS. Two micrograms of biotinylated antibody (antiCD91#ab20384; abcam) was added and mixed gently. The mixture was incubated at room temperature for 1 h with slow tilt rotation. The beads were washed three times with PBS to remove the unbound antibodies and finally the antibody-bead complex (functionalized beads) was resuspended in 400 µl PBS and stored on ice.

The stock of frozen EVs suspension at −20 °C was thawed on ice, and 28 µl was mixed with 400 µl of the CD91-immunomagnetic bead solution and incubated overnight at 4 °C with gentle tilt rotation. The captured CD91 positive exosomes by beads were separated from the solution using magnetic separation. Captured beads were washed three times with PBS and stored at −20 °C. Further to elute the captured exosomes from magnetic beads, 100 µl of 0.1 M Glycine HCl (pH 2.6) was added to the exosome-bead solution and incubated on ice for 10 min then centrifuged at 4500×g for 10 min at 4 °C. The pH was neutralized by adding 10 µl of 1 M Tris-HCl (pH 8.5) to the supernatant. The eluted exosomes were concentrated using 100 KDa MWCO nanosep centrifugal device (cat. # 88533 Thermo scientific).

2.7. Total protein and Western blot assay

Total Protein concentrations of EVs obtained at 100,000 g or 20,000 g centrifugation fractions were measured by using a BCA protein assay kit (Thermo fisher scientific, #23225) according to manufacturer's instructions. Briefly, equal volume of each exosomal fraction was homogenized with 1x RIPA buffer (# 89900; Thermo fisher scientific) containing protease inhibitor and lysed with 4X Laemmli buffer (BIO-RAD) under reducing conditions and denatured at 95 °C for 10 min. The

soluble protein extracts were loaded and run into Mini protean pre-cast gel (10%, BIO-RAD #456–1033), then transferred onto PVDF membranes. Membranes were blocked using clear milk blocking buffer (Thermo fisher scientific) in Tris-buffered saline containing 0.1%Tween 20 for 1 h followed by overnight incubation at 4 °C with primary antibodies specific for CD63 (# ab134045, abcam), CD81 (# ab59477, abcam) and lung cancer marker CD91 (# ab20384, abcam). Antibodies to β-actin (# ab8227, abcam) and GAPDH (# ab8245 abcam) were used as loading controls. After 1-h incubation at 4 °C with Goat anti-mouse IgG (H + L) poly HRP (# 32230; Thermo fisher scientific) and Goat anti-rabbit IgG (H + L) poly HRP (# 32260; Thermo fisher scientific) secondary antibodies, membranes were developed by Super signal west Pico plus chemiluminescent substrate (Thermo fisher scientific). Images were acquired using the L1-COR Gel scanner, and images were analyzed using NIH ImageJ software.

2.8. Biophysical characterization of EVs

The hydrodynamic size of EVs size was determined by Dynamic Light Scattering (DLS) using zetasizer Nano ZSP particle sizer (ZEN5600; Malvern Panalytical Limited, Worcestershire, UK). For particle sizing in solution, EVs were diluted in 1x PBS and 10 µl of sample was loaded in sub-micro Quartz cuvette, measurements were obtained in triplicates at constant temperature of 24 °C. Results were exported into text file and graph was plotted using Prism Graph pad software.

Transmission electron microscopy (TEM) and Immunogold Labeling: The morphology of EVs isolated at 100,000 g or 20,000 g centrifugation were observed by TEM imaging. In addition, morphology of CD91 positive exosomes eluted from magnetic bead assay and presence of CD91 on their membrane was characterized by immune-gold TEM. The captured exosomes were first eluted from the beads by adding 0.1 M Glycine HCl (pH 2.6), mixed for 10 min on ice and centrifuged at 4500×g for 10 min at 4 °C. The pH was neutralized by adding 1 M Tris-HCl (pH 8.5). The eluted exosomes were concentrated using 100KD nanosep centrifugal device and resuspended in PBS. The immunolabeling for the eluted exosome was carried as described previously with some modifications [33]. Briefly, a 5 µl drop of eluted exosomes was coated on a Formvar/carbon 200 mesh copper grid (Ted Pella, Inc.) and adsorbed for 20 min. The sample was fixed by depositing a drop of fixative mixture containing 4%Glutaraldehyde and 2% Formaldehyde for 7 min. The grid was washed 3 times with PBS, followed by blocking for 10 min in 5% BSA before immunostaining. Electron microscopy was also performed without immunostaining to identify size and morphology of total exosomes derived from cell culture and plasma samples of patients and these samples were negatively stained with 0.2% uranyl acetate. For immunostaining, a 5 µL drop of CD91 antibody (#ab20384; abcam) in 5% BSA was adsorbed on the TEM grid containing adsorbed exosomes and incubated for 1 h at 4 °C. The free antibody was removed by washing three to five times with PBS buffer and the secondary goat anti-mouse IgG-10nm gold-labelled antibody (#ab 39619; abcam) was added to the grid for 30 min. The grid was washed 3 times with PBS and the immunoreaction was post-fixed again with 4% glutaraldehyde and 2% formaldehyde mixture for 5 min. Post washing, sample was dehydrated using 50%,70%,80%,90% and 100% ethanol gradient solutions, first air-dried for an hour then stored in vacuum desiccator until imaging on transmission electron microscope (TEM-FEI, Talos-F200x).

2.9. Immunohistochemistry of lung cancer biopsy tissue

Paraffin-embedded sections (4µm thick) of human lung cancer patients with known fixation history (10% neutral buffered formalin, 18–24 h) were obtained from the department of pathology, Hamad medical corporation (HMC). The paraffin-embedded sections (4 µm thick) were dewaxed and rehydrated. After rehydration the antigen retrieval was done in antigen retrieval buffer (Tris/EDTA pH 9.0) The endogenous peroxidase activity was blocked in 3% H₂O₂ after the

antigen retrieval. Sections were washed in water and TBS Triton (0.01%) and were blocked in blocking buffer (5% Normal goat serum in Antibody diluent (#Cell Signaling Cat. # 8112 L) for 1 h at room temperature followed by incubation with primary antibody (#ab20384; abcam) at 1:250 dilution in a humidified chamber at 4° overnight. After the primary antibody incubation, sections were washed thrice in TBS Triton (0.01%) to remove unbound antibody, followed by incubation for 1 h at room temperature with appropriate horseradish peroxidase-conjugated secondary antibody. Immunoreactive complexes were detected using 3,3'-diaminobenzidine (DAB) (#Dako Corp., Carpinteria, CA). Slides were then counterstained in hematoxylin, mounted in crystal mount. Sections were visualized on a Nikon ECLIPSE Ni-U upright microscope and Images were captured with an attached DS-Ri1 camera and later processed with ImageJ Software NIH. Images were analyzed for Allred score by analyzing proportion score (PS) in the range of 0–5 were 0 = negative 1 = weak and 5 = strong. The Intensity score (IS) 0–3, 0 = negative, 1 = weak and 3 = strong, Allred score = PS + IS. The analysis was carried from five slides, each slide cells were analyzed full field of view (FOV) containing 100–120 cells. Similarly, immunofluorescence imaging was performed by adding FITC labelled secondary antibody instead of horseradish peroxidase-conjugated secondary antibody. Slides were washed and kept in dark. Fluorescence images were obtained by Olympus IX73 inverted microscope attached with Xyla 4. Andor camera. 60X objective was used. Images were calibrated with ImageJ software. Cell counting and fluorescence maximum intensities

from each single cell from a FOV containing 150 cells was measured using plug-in cell counter of the Image-J software, all measurements were plotted in Prism Graph pad 9. Intensities were grouped into weak, intermediate, and strong similar to IS score of Allred.

2.10. Statistical analysis

Statistical analysis was performed with GraphPad Prism 9 software, All experiments were performed in triplicates. The significance was determined by unpaired *t*-test with Welch's correction. Western blots were cropped and processed in image J software for densitometry measurements. The integrated mean intensities of CD91 from each single cell, N = 10, were measured from LL-24, NCI-H1975, MCF-10A, and MCF-7 florescent microscopic images using ImageJ software, and significance unpaired *t*-test with Welch's correction was performed. All western blots were performed in triplicates. The analysis of western blots of EVs from plasma were normalized by total protein of EVs or with their respective CD63.

Final figures were prepared in EazyDraw software, license version 10.5.3.

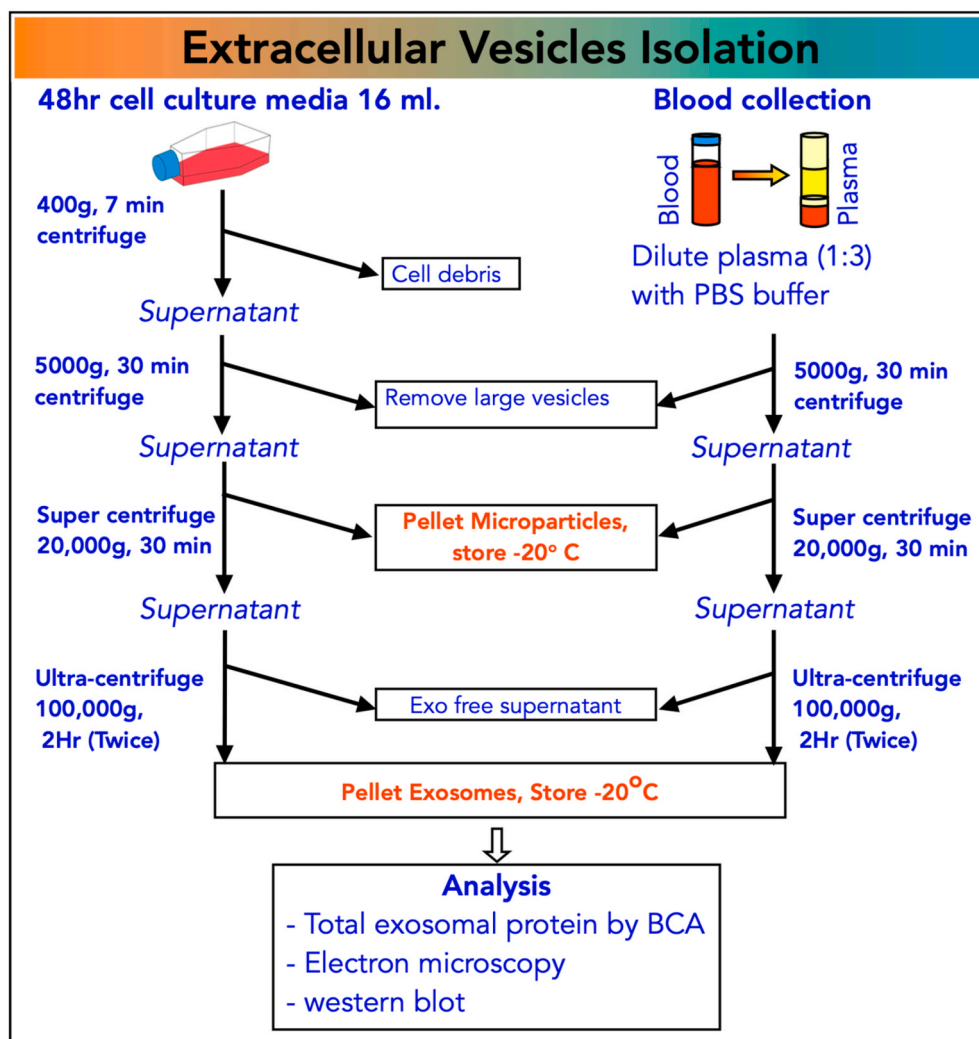


Fig. 1. Schematic representation of EV Isolation from cell culture and plasma samples.

3. Results

3.1. Expression of CD91 biomarker in cell lines

To evaluate the expression of CD91 in extracellular vesicles, we first sought to determine the expression of CD91 in lung cancer cells. Therefore, we performed immunofluorescence imaging in fixed cells, and our results show that NCI-H1975 cells enormously expressed CD91, as shown in Fig. 2, and the analysis of fluorescence intensities determine

that CD91 is significantly over expressed in NCI-H1975 comparing to LL24 or MCF-10A or MCF-7 shown in Fig. 2e. In addition, microscopic images showed that breast cancer cell line (MCF-7) and breast non-malignant epithelial cells (MCF-10A) also showed moderate expression of CD91 (Fig. 2c and d), however the analysis of fluorescence intensities show that most of MCF-10A cells did not express CD91, and those cells expressing CD91 was only seen as cytosolic. Similarly, normal lung epithelial cells (LL-24) showed deficient expression of CD91 in the cytosol and were explicitly not seen in the membrane (Fig. 2d). Our

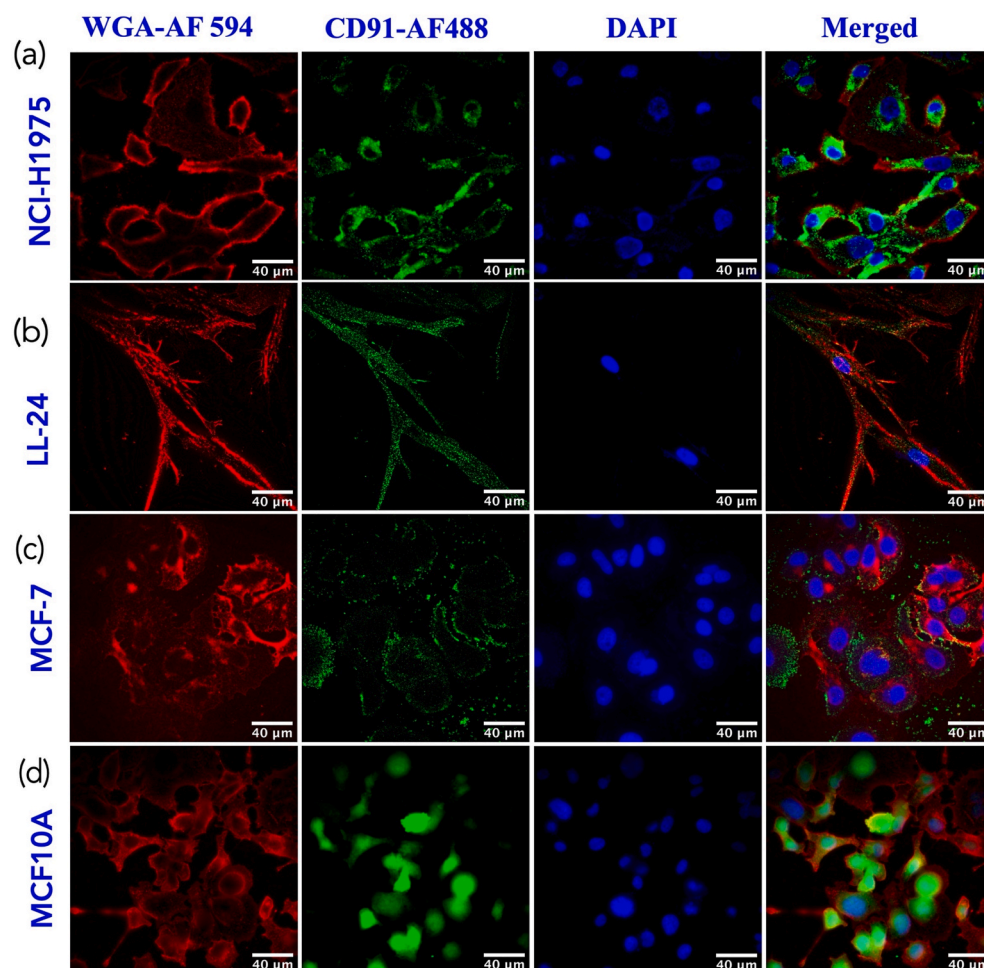
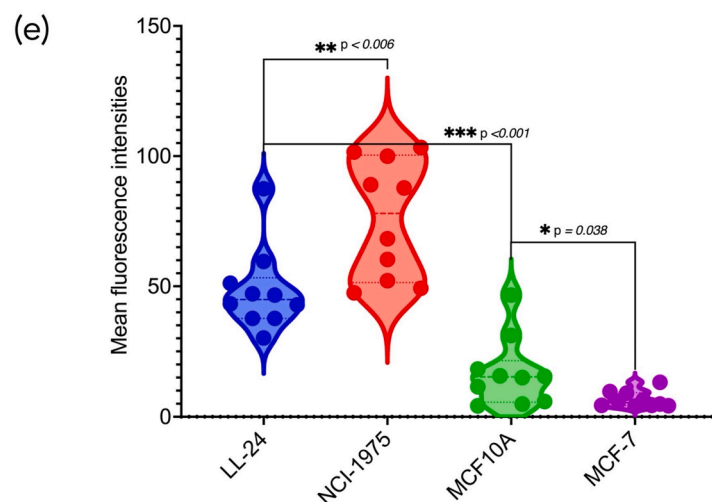


Fig. 2. Immunofluorescence microscopy determining CD91 expression in cell lines: Representative images of para-formaldehyde fixed cells: (a) NCI-H1975 (NSCLC cells) (b) LL-24 (Normal Lung cells) (c) MCF-7 (Breast cancer cells) (d) MCF-10A (Non -malignant breast cells). Cells were nuclei stained with DAPI (blue), plasma membrane stained with wheat germ agglutinin (WGA) conjugated with Alexa Fluor 594 dye (AF-594) (red), and antiCD91 targeted secondary antibody conjugated with Alexa Fluor-488 (green). (e) Representing analysis of CD91 expression, the bar graph showing mean \pm S.D. of integrated fluorescence intensities, $N = 10$, measured in triplicates. Images were taken with fluorescent inverted microscope Olympus IX73 \times , 60 \times objective of NA 1.4, images were captured with CCD camera Zyla 4.2 Andor USA. The length of scale bar in each image is 40 μ m. (For interpretation of the references to colour in this figure legend, the reader is referred to the Web version of this article.)



results also determine that cancer cells NCI-H1975, and MCF-7 showed expression of CD91 primarily localized in the membrane, and while as non-cancerous cells MCF-10A and LL-24 showed a fair expression of CD91 mainly in the cytosol.

3.2. Expression of CD91 biomarker in NSCLC tissue biopsy

Lung biopsy tissues showed expression of CD91 which was determined by immunofluorescence (Fig. 3-A and B), results showed CD91 was largely expressed in NSCLC biopsy tissue and seen as cytosolic and on membrane as well. The intensity score of CD91 fluorescence showed

56.5% of cells were high score as shown in Fig. 3-F and 3G. Furthermore, we confirmed CD91 expression in lung biopsy tissue by immunohistochemistry (Fig. 3-D), and the analysis determined the Allred score of 7.2 as shown in Fig. 3-E. To check the tissue integrity and histopathological conditions, the hematoxylin and Eosin (H&E) staining was performed which showed infiltration of white blood cells in tissues (Fig. 3-C).

3.3. EVs expressing CD91 derived from NCI-H1975 cells and non-cancerous cells

Further to evaluate the CD91 in extracellular vesicles, we isolated

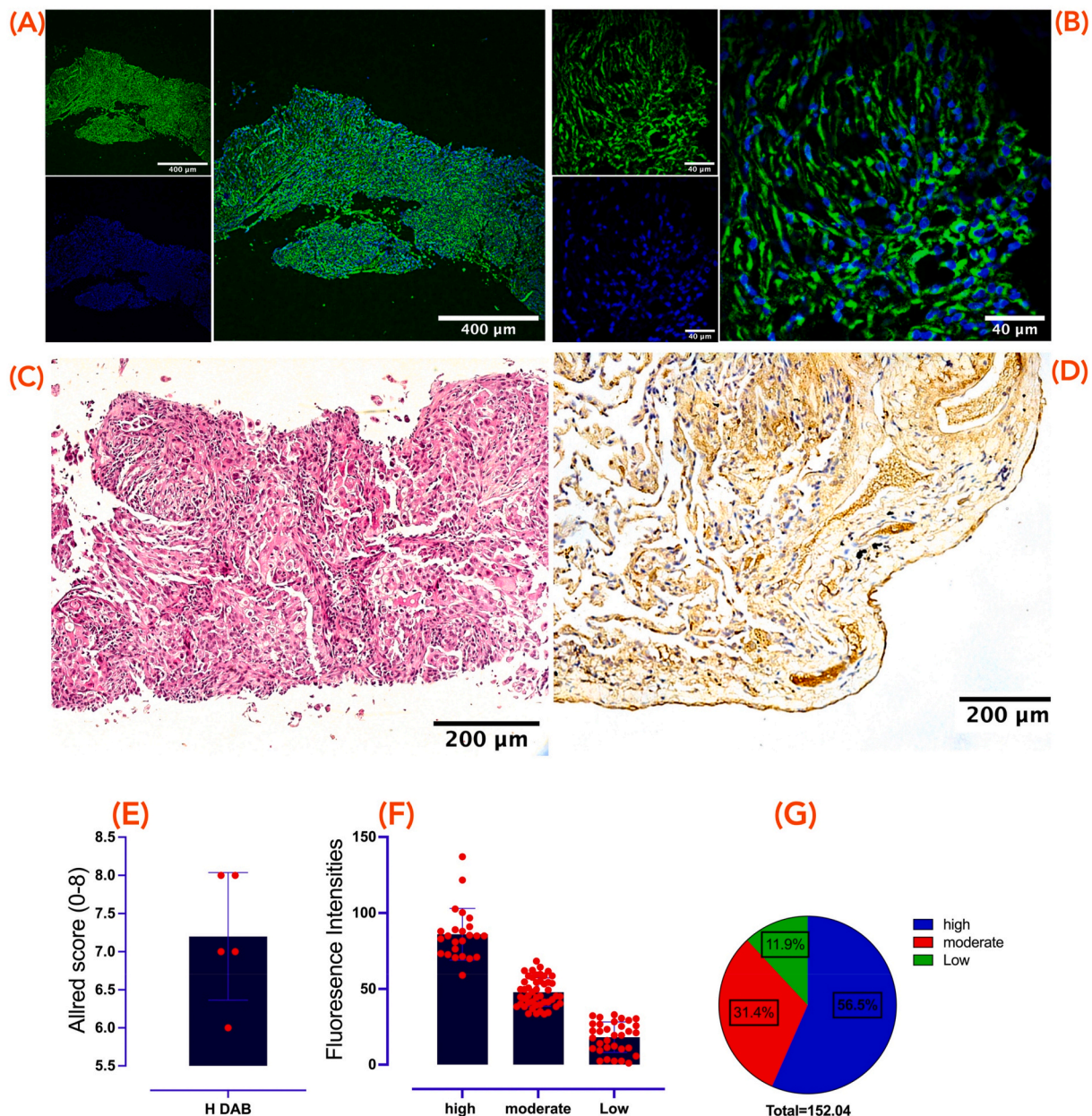


Fig. 3. Immuno-fluorescence and immunohistochemistry of lung cancer biopsy tissue.

Characterization of CD91 in Lung Biopsy tissue, (A) and (B) micrographs representing FITC labelled anti-CD91 (green), and nuclear stain DAPI (blue), images were taken with 10X and 60X objective, each image having a measuring scale bar 400 μ m and 40 μ m respectively. (C) Hematoxylin and Eosin staining of NSCLC tissue, images were taken with 20X objective. (D) DAB immunohistochemistry shows expression of CD91 in NSCLC biopsy tissue. (E) Analysis of CD91 expression in immunohistochemistry images, the bar graph representing mean \pm SD of the Allred score, N = 5 slides from 5 different patients. (F) Analysis of CD91 expression from immunofluorescence images, each bar graph representing mean \pm SD of intensity score (IS) measured from each single cell, total number of cells N = 150. (G) Parts of whole graph representing the percentage of IS among three groups. Immunohistochemistry was performed from five patients. In each microscopic tissue slide, images were captured from at least three different XY planes. (For interpretation of the references to colour in this figure legend, the reader is referred to the Web version of this article.)

extracellular vesicles (EVs) from cell culture media of growing cultures of lung cancer cell line NCI-H1975 and non-malignant cell lines including normal lung cells LL-24 and non-malignant breast cell line MCF-10A. EVs were isolated using standard protocol of ultracentrifugation. The biophysical characterization of EVs from NCI-H1975 using DLS showed EVs isolated from ultra-centrifugation have heterogeneous size, the histogram showed maximum peak height approximately at 78.8 nm (Fig. 4A). However, it was obvious from the data that EVs show aggregation, because prior to ultra-centrifugation microparticles were removed by centrifugation at 20,000 g which are usually 200 nm to few microns in diameter. Hence, we believe that large size of EVs by DLS analysis may be because of aggregation. We also measured size of microparticles (MPs) isolated at 20,000 g using DLS analysis, and our results show sizes were heterogeneous and the maximum peak height was observed at 295 nm (Fig. 4B), which is higher than 100,000 g EV (exosomes). Exosome morphology and size was further characterized by transmission electron microscopy that showed the vesicles of varied sizes from 30 to 120 nm in diameter and rounded shape with defined membrane as shown in (Fig. 4C). The TEM image of MPs shows mostly large size 200–300 nm with well-defined membranes like exosomes (Fig. 4D).

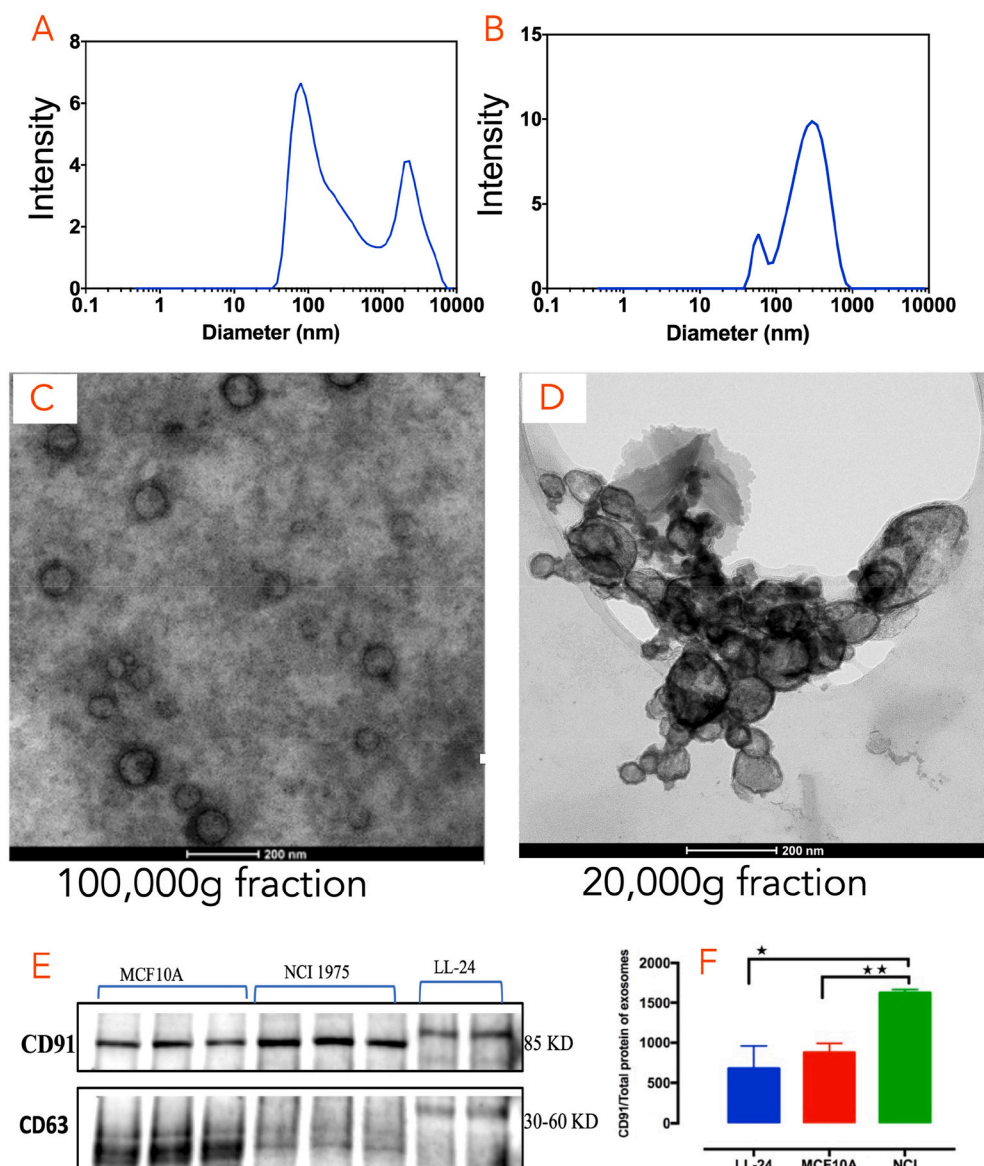
Furthermore, EVs general marker [34] CD63 was characterized by western blotting in NCI-H1975, LL24 and MCF-10A, however the expression of CD63 was higher in MCF-10A, and in addition CD91 was also observed in EVs from all three cell lines and was observed as significantly higher in lung cancer NCI-H1975 cells. Interestingly we observe CD63 and CD91 slightly higher molecular weight in LL24 comparing to NCI-H1975 and MCF-10A, we think this could be attributed to the effect from posttranslational modification and difference in glycosylation (Fig. 4E). These results demonstrate that CD91 was over expressed in EVs from NCI-H1975 (Fig. 4F).

3.4. Determine CD91 in exosomes versus microparticles

Cell culture isolated EVs consist of heterogeneous sizes and are mainly categorized in two subgroups: (1) MPs isolated at 20,000 g centrifugation are also considered as source of biomarkers [35], (2) exosomes isolated by ultracentrifugation fraction at 100,000 g. Thus, to investigate whether CD91 is present in MPs and exosomes, we purified MPs and exosomes from cells cultured in serum free media (NCI-H1975, MCF-10A and MCF-7) at 20,000×g and 100,000×g centrifugation respectively. Furthermore, western blots were employed to demonstrate

Fig. 4. EV validation and CD91 characterization in total exosomes from NSCLC and normal cell lines.

Validation of invitro EV isolation and characterization of CD91 in exosomes. (A) and (B) showing dynamic light scattering (DLS) measurements as Intensity plots of particle size distribution in exosomes and microparticles (MPs) derived from NSCLC cells, respectively. (C, D) Transmission electron microscopy (TEM) image of exosomes (100,000 g fraction) and MPs (20,000 g fraction) derived from NCI-H1975 cell culture. (E) Western blot images showing exosome enriched protein in CD63 and CD91 in MCF-10A NCI-H1975, and LL-24) cells. (F) The Western blot bar graph of the densitometry representing the expression of CD91, each bar is mean \pm standard error, N = 3, The analysis showing CD91 normalized to total protein in exosomes. The unpaired t-test with Welch's analysis showing the significance p values as *P < 0.05, and **p < 0.01.



the expression of CD63 and CD91 in both the centrifugal fractions. However, LL24 cells could not be continued in this study because we have limited stock of cells, these cells are non-transformed normal healthy lung fibroblasts and do not grow more than 3 to 4 passages, as a result we could not expand the cell number.

Our results show that the CD63 was detected in both the exosomes and MPs isolated from three types of cell lines (Fig. 5A and B). Next, we analyzed CD91, our results show that MPs did not express CD91 and was observed in all three cell lines (Fig. 5B), while as exosomes showed expression of CD91 derived from MCF-10A and NCI-H1975 cells, however Western blot of exosomes from MCF-7 cells show negligible expression of CD91. Among MCF-10A and NCI-H1975 cells, CD91 was significantly expressed more in NCI-H1975 (Fig. 5A, C).

3.5. Characterization of CD91 in plasma derived EVs

To determine the expression of CD91 in EVs from plasma of lung cancer patients and age matched healthy group, we obtained plasma samples of NSCLC from National Centre for Cancer Care and Research (NCCCR), HMC, Qatar. EVs were successfully isolated from plasma samples by using ultracentrifugation as outlined in Fig. 1. Further, EVs of both the centrifugal fractions were characterized by Dynamic Light scattering (DLS), results showed the average size of exosomes population was 142 nm as shown (Fig. 6A) while as MPs average size was approximately 825 nm (Fig. 6B). However, exosomes and MPs showed multiple peaks in histogram which may reflects diversity in size and possibly larger size could be related to aggregation. Next, western blotting was performed to detect EVs general marker CD63 in both the centrifugal fractions of EVs as shown in Fig. 6-C and 6-D. Furthermore, we aim to detect EV general marker CD63 and CD91 among NSCLC patients and healthy group. The differential expression of CD91 and CD63 in exosomes is shown in bar graphs Fig. 6E and F, the fold change difference was statistically non-significant. Furthermore, we normalized

CD91 to its respective EV general marker CD63 and the fold change in CD91 was plotted as shown in Fig. 6G. Our results demonstrate that CD91 expression was significantly higher in NSCLC compared to healthy groups. Normalizing densitometry scan of biomarkers from EV's has been challenging, however it is well known that CD63 is a general biomarker of EV's and it is suggested CD63 can be used instead of GAPDH [36]. Next, we showed the differential expression of CD91 and CD63 in MPs as shown in Fig. 6H, I and 6J, the results demonstrate that CD91 fold change when normalized to its total protein of EVs was significantly higher in MPs, while as CD63 expression was non-significant in MPs. Moreover, the CD91 differential expression in MPs when normalized by its CD63 was statistically significant.

3.6. Validation of CD91 in exosome sub-population

Further to characterize specific population of EVs expressing CD91 from NSCLC plasma, we used immunocapture bead assay technique. Since the expected localization of CD91 is on the surface of exosomes, biotinylated anti-CD91 antibody conjugated with streptavidin magnetic beads was utilized as an exosome capture antibody. The captured CD91 exosome sub-population was eluted from the beads, and were characterized by DLS, TEM imaging and Western blot to confirm EV's specific general markers.

Morphologically, the eluted exosomes from beads were spherical in shape, and were within the range of size of exosomes as observed in TEM images (Fig. 7A). DLS analysis showed that the average size of these CD91 pulled exosomes were approximately 68.1 nm, (Fig. 7D). Furthermore, to demonstrate that CD91 a membrane protein is located on EV membrane, we performed immuno-gold staining for TEM imaging. Our results confirmed that CD91 is expressed on exosome surface by immunogold staining for CD91, verifying that NSCLC exosome sub-population have CD91 on their membrane surface (Fig. 7B and C). EVs eluted from CD91 beads without immunogold staining shown in Fig. 7A.

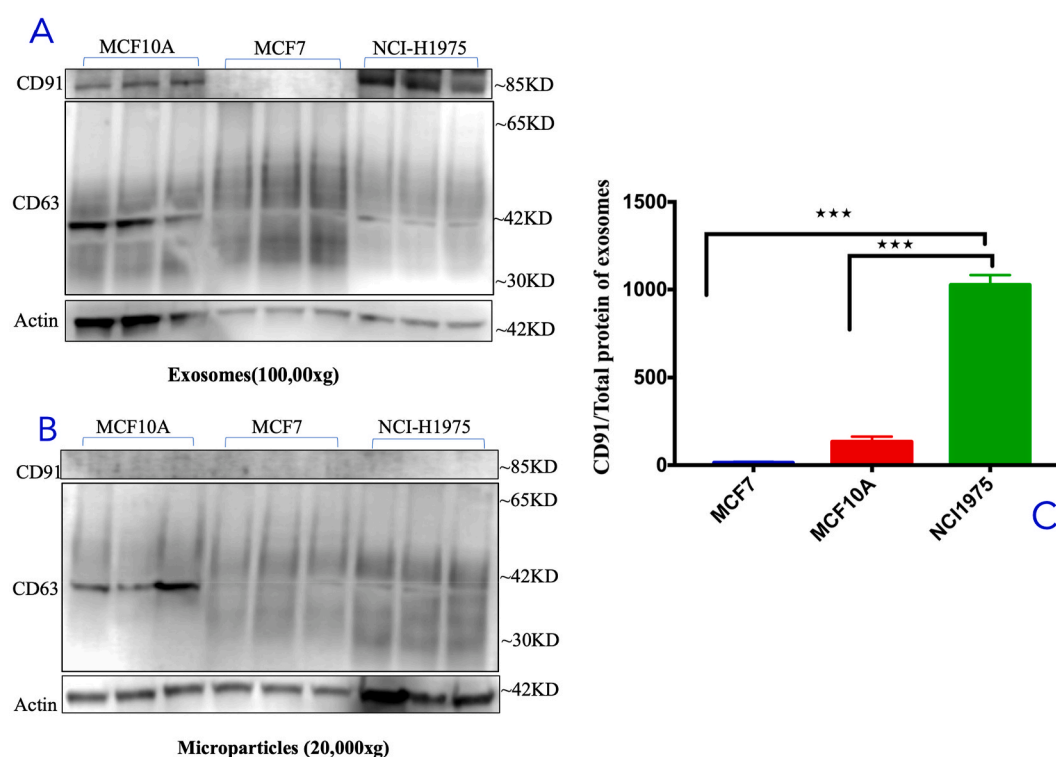


Fig. 5. Western blot analysis of exosomes and microparticles obtained from cell culture supernatants. The general EV marker CD63 and NSCLC marker CD91 was investigated in exosomes or MPs isolated from MCF-10A, MCF-7 and NCI-H1975 cell cultures. (A) and (B) Western blots showing CD63, CD91 and actin in exosomes and MPs respectively. (C) Densitometry analysis of exosomes shown in bar graph, each bar is mean \pm SD, N = 3. The statistical analysis by Welch's unpaired *t*-test, P value represented as * <0.05 , ** <0.01 , and *** <0.001 .

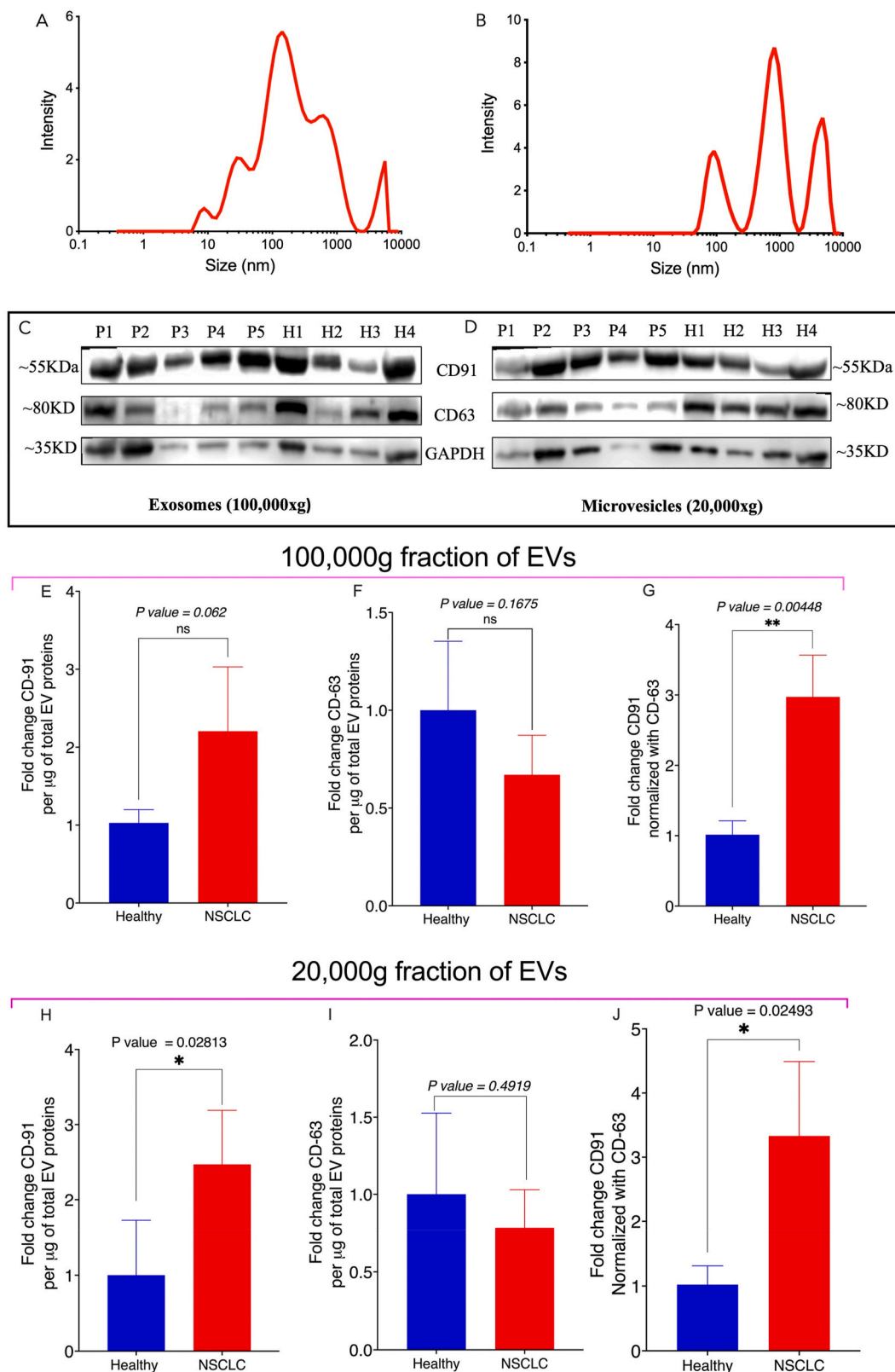


Fig. 6. Biophysical characterization of EVs derived from plasma. (A) and (B) representing the DLS analysis of the hydrodynamic size distribution of plasma derived exosomes (100,000 g fraction) or microparticles (20,000 g fraction) respectively, each analysis was performed in triplicates. (C–D) Western blots showing expression of CD91 (MW~55 KDa), CD63 (MW ~70–80 KDa) and GAPDH (MW~35 KDa) in exosomes or microparticles respectively. (E, F, and G) graphs showing densitometry results from western blots of exosomes, (H, I, and J) graphs showing the densitometry results from Western blot of microparticles. Each bar in graph is mean \pm SD, $N = 4$ for healthy group and $N = 5$ for NSCLC group. The significance among the groups shown as unpaired t -test, with Welch's correction; * represents p value < 0.05 and ** P value < 0.01 .

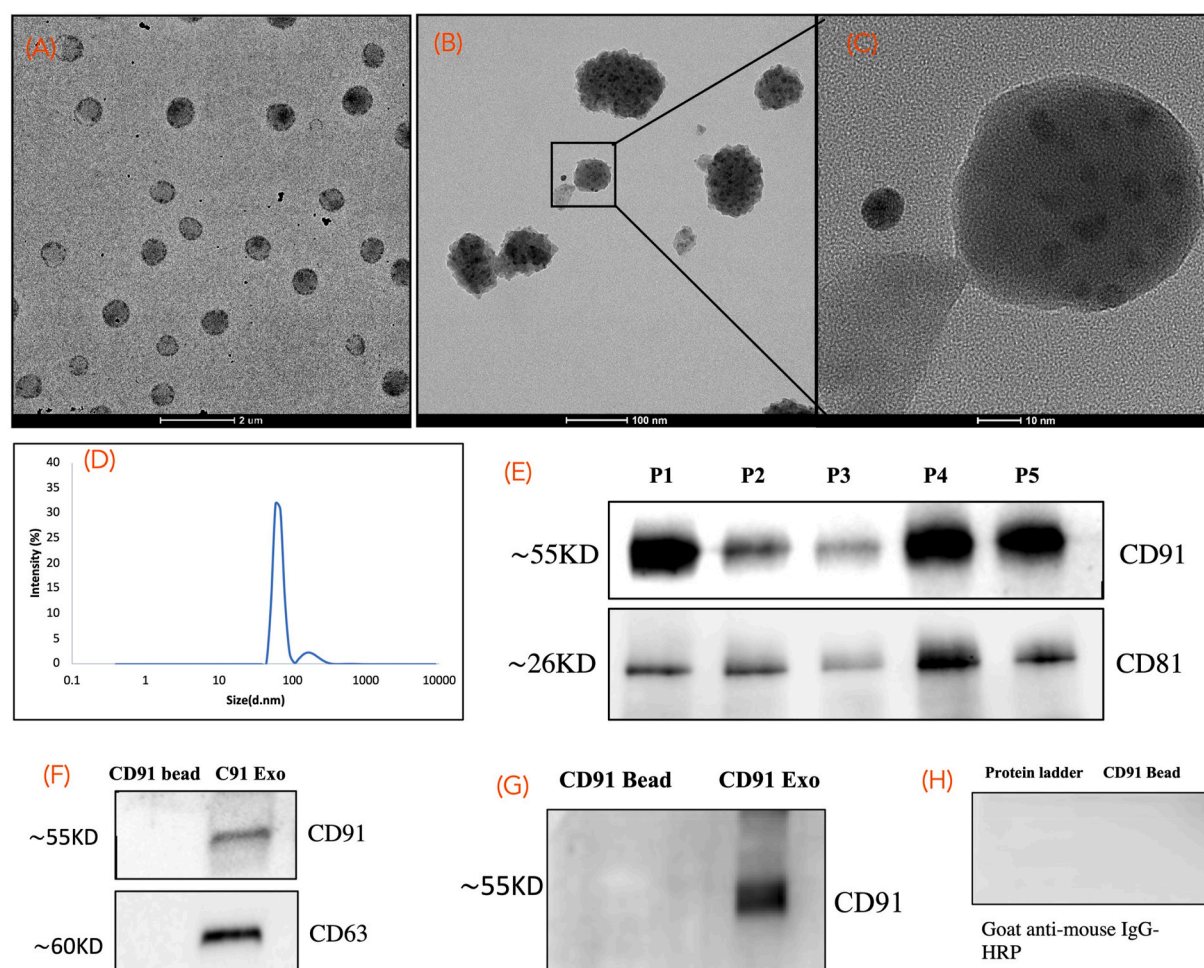


Fig. 7. Characterization of CD91 positive exosome isolated from NSCLC plasma samples.

(A) TEM image of NSCLC plasma derived exosomes after eluted from CD91 capture beads. (B) TEM image of immunogold stained CD91-pulled exosomes labelled with 10 nm gold nanoparticles showing gold nanoparticles bound to EVs. (C) Zoom image from inset placed in figure B. (D) Size distribution by DLS (Malvern) of CD91 positive exosomes eluted from capturing beads. (E) Western blot analysis of exosomal protein CD81 and confirmation of CD91 in the NSCLC exosome sub-population. (F) Detection of CD63 and CD91 exosomal marker in the CD91-pulled exosomes. (G) Western blot analysis of CD91-functionalized bead and CD91-pulled exosomes using anti-CD91 antibody. (H) Western blot analysis of CD91-functionalized bead probed directly with secondary anti-mouse antibody. (For interpretation of the references to colour in this figure legend, the reader is referred to the Web version of this article.)

The eluted EVs from the CD91 captured beads were further analyzed by Western blot for CD91 and CD81 as shown in figure (Fig. 7E), the EVs were isolated from five NSCLC patients (P1 – P5). To eliminate the doubt of cross-contamination of capturing bead and capturing antibody, negative controls were run that confirmed the CD91 expression is indeed from the EVs not from captured antibody (Fig. 7G). In another control as shown in (Fig. 7H), beads functionalized with anti-CD91 were immunoblotted and probed directly with secondary antibody without EV's, showed no bands. Further we demonstrated that CD91 pulled EVs does express CD63 (Fig. 7F), in this control, we probed with antiCD91 or antiCD63 to CD91 bead pulled exosomes. All these findings demonstrated that CD91 is a membrane protein on EVs.

4. Discussion

Studies have suggested that EVs may be valuable diagnostic biomarkers for several cancers, including lung cancer [11]. Pan, D. et al. Reported the proteomics analysis of plasma-derived exosomes in NSCLC patients and found CD91 was expressed 5-fold more when compared to healthy controls [31], and these results indicate that plasma-derived EVs expressing CD91 may have potential as a diagnostic marker for NSCLC. In addition, a mass spectrometric quantification study of exosomal

proteins confirmed CD91 from NSCLC exosomes [37]. CD91 is a multi-functional scavenger and signaling receptor that belongs to the LRP family [38]. Several reports suggest that CD91 expression is weak in various cancer cell lines and tissues, thus assigning a tumor-suppressive role to this receptor [32,39–42]. Besides, evidence suggest a role for CD91 in thyroid cancer cell metastasis [43–45], and as predictive of more aggressive tumor of endometrial carcinomas [46]. Contrarily the expression of CD91 in dendritic cells plays a role in priming T-cells against cancer cells to produce CD4 and CD8 [47,48]. These contrasting features of CD91 in cancer or healthy immune cells suggest more study is needed to unveil its mechanism of function in cancer cells. To our knowledge, the expression of CD91 in lung cancer cells has not been fully investigated. To correlate the elevated expression of CD91 in EVs as diagnostic biomarker of NSCLC cancer, this study confirms that CD91 is over expressed by lung cancer cells and is carried by extracellular vesicles.

In the present study, our invitro results confirm that CD91 is expressed in the NSCLC cell line, (Fig. 2), and also confirmed expression of CD91 in NSCLC tumor biopsies (Fig. 3). Although from earlier studies it was known that CD91 is higher in plasma or serum of lung cancer patients, but this study confirms that the overexpression of CD91 may be contributed by the tumor lung cells in addition to immune cells. Further

the question remained if EVs containing CD91 are contributed from tumor lung cancer cells, our findings determine that CD91 in EVs from serum are also contributed from the lung tumor NSCLC patients. The biophysical characterization of EV's from our invitro analysis determine that only exosomes, carried CD91 compared to MP's (Fig. 5.). These results demonstrated selective group of EV's may be containing CD91. Circulating EV's in blood represent EV's contributed from whole body tissues particularly blood cells. Thus, to isolate EV's we used similar centrifugation technique as in invitro as shown in Fig. 1 to separate EVs from the plasma of NSCLC patients and age matched healthy controls. In contrast to invitro data, plasma derived MPs and exosomes both showed CD91 expression in NSCLC patients and healthy controls, the differential expression of CD91 was significantly higher in NSCLC patients MP's and exosomes. However, it was worth noting that MPs from cell culture did not show CD91 in our Western blot results. We believe in the plasma CD91 positive EVs are contributed from several other tissues mainly dendritic cells [49] suggesting that CD91 packaging in EVs will depend on their function and origin. Therefore, CD91 in exosomes could reflect more accurate diagnostic marker in NSCLC patients comparing to CD91 in MP's. Hence, it will be important to study the role of CD91 in exosomes and MPs to demonstrate if polymorphism in CD91 distinguishes among exosomes or MPs.

The study of protein markers from EVs is constantly questioned about the cross contamination from circulating plasma soluble proteins [30,50]. However, our immunogold staining in TEM images confirmed that CD91 is certainly present in plasma derived EVs.

In recent years, ultracentrifugation has been used as the most common technique to purify exosomes. However, it cannot remove aggregated circulating proteins in the plasma due to their similar diameters and sedimentation coefficient to exosomes [30,50]. To overcome these contaminants, we employed an immunocapture bead assay technique to isolate and characterize the specific population of NSCLC exosomes. Recently, it was shown that L1CAM expression in EVs is observed as cross-contamination and is present only as a soluble protein in plasma [51]. Hence to prove CD91 is a membrane-bound protein in EVs, we used magnetic bead assay to separate EVs, and further confirmed CD91 on EVs by TEM immunogold staining. We believe this is the first study showing expression of CD91 in lung cancer cells, NSCLC tumor tissue, and conforming CD91 in EVs. This study may benefit biomarker studies in NSCLC disease. This pilot study has limitations in determining significant differences in CD91 expression in EV's among NSCLC patients and healthy controls because of small population size, thus a future study of large population will be needed to quantitatively analyze CD91 in cancer patients and healthy groups. This suggests further proteomic study is needed to determine if polymorphisms of CD91 may exist among lung cancer cells and extracellular vesicles which will contribute to the development of cancer diagnosis and prognosis biomarkers.

5. Conclusion

Our preliminary findings suggest that CD91 is significantly expressed by NSCLC cells and is also found in EVs derived from NSCLC cells. In addition, we also confirmed higher expression of CD91 in lung cancer biopsy tissues and in exosomes of NSCLC patients. Therefore, we believe EV's expressing CD91 may play a critical role in biomarker studies in the diagnosis and prognosis of NSCLC patients. Further studies are needed to determine the function of CD91 positive EVs in NSCLC patients.

Declaration of competing interest

The authors declare that they have no known competing financial interests or personal relationships that could have appeared to influence the work reported in this paper.

References

- [1] Cancer. <https://www.who.int/news-room/fact-sheets/detail/cancer>.
- [2] N. Duma, R. Santana-Davila, J.R. Molina, Non-small cell lung cancer: epidemiology, screening, diagnosis, and treatment, *Mayo Clin. Proc.* (2019) 94 1623–1640.
- [3] U. Testa, G. Castelli, E. Pelosi, Lung cancers: molecular characterization, clonal heterogeneity and evolution, and cancer stem cells, *Cancers* 10 (2018) 248.
- [4] P. Goldstraw, et al., The IASLC lung cancer staging project: proposals for revision of the TNM stage groupings in the forthcoming (eighth) edition of the TNM classification for lung cancer, *J. Thorac. Oncol.* 11 (2016) 39–51.
- [5] Team, T. N. L. S. T. R., Reduced lung-cancer mortality with low-dose computed tomographic screening, *N. Engl. J. Med.* 365 (2011) 395.
- [6] H. De Koning, C. Van Der Aalst, K. Ten Haaf, M. Oudkerk, PL02.05 effects of volume CT lung cancer screening: mortality results of the NELSON randomised-controlled population based trial, *J. Thorac. Oncol.* 13 (2018) S185.
- [7] B. N, et al., Lung cancer mortality reduction by LDCT screening-Results from the randomized German LUSI trial, *Int. J. Cancer* 146 (2020) 1503–1513.
- [8] U. Pastorino, et al., Prolonged lung cancer screening reduced 10-year mortality in the MILD trial: new confirmation of lung cancer screening efficacy, *Ann. Oncol.* 30 (2019) 1162.
- [9] P. Pf, et al., Performance of lung-RADS in the national lung screening trial: a retrospective assessment, *Ann. Intern. Med.* 162 (2015) 485–491.
- [10] B.H.L. Goulart, S.D. Ramsey, Moving beyond the national lung screening trial: discussing strategies for implementation of lung cancer screening programs, *Oncol.* 18 (2013) 941.
- [11] G. Rabinowitz, C. Gerçel-Taylor, J.M. Day, D.D. Taylor, G.H. Kloecker, Exosomal microRNA: a diagnostic marker for lung cancer, *Clin. Lung Cancer* 10 (2009) 42–46.
- [12] G. van Niel, G. D'Angelo, G. Raposo, Shedding light on the cell biology of extracellular vesicles, *Nat. Rev. Mol. Cell Biol.* 19 (2018).
- [13] M. Mathieu, L. Martin-Jaulat, G. Laviue, C. Théry, Specificities of secretion and uptake of exosomes and other extracellular vesicles for cell-to-cell communication, *Nat. Cell Biol.* 21 (2019).
- [14] J.M. Nikoloff, M.A. Saucedo-Espinosa, A. Kling, P.S. Dittrich, Identifying extracellular vesicle populations from single cells, *Proc. Natl. Acad. Sci. U. S. A.* 118 (2021).
- [15] M. Colombo, G. Raposo, C. Théry, Biogenesis, secretion, and intercellular interactions of exosomes and other extracellular vesicles, *Annu. Rev. Cell Dev. Biol.* (2014) 30 255–289.
- [16] N.P. Hestvik, A. Llorente, Current knowledge on exosome biogenesis and release, *Cell. Mol. Life Sci.* (2018) 75 193–208.
- [17] B. Sandfeld-Paulsen, et al., Exosomal proteins as diagnostic biomarkers in lung cancer, *J. Thorac. Oncol.* 11 (2016) 1701–1710.
- [18] P. Reclusa, et al., Exosomes as diagnostic and predictive biomarkers in lung cancer, *J. Thorac. Dis.* (2017) 9 S1373–S1382.
- [19] S. Taverna, et al., Exosomes isolation and characterization in serum is feasible in non-small cell lung cancer patients: critical analysis of evidence and potential role in clinical practice, *Oncotarget* 7 (2016) 28748–28760.
- [20] W. Wang, et al., The crosstalk: exosomes and lipid metabolism, *Cell Commun. Signal.* 18 119 (2020).
- [21] R. Wubbols, et al., Proteomic and biochemical analyses of human B cell-derived exosomes: potential implications for their function and multivesicular body formation, *J. Biol. Chem.* 278 (2003) 10963–10972.
- [22] S. Boukouris, S. Mathivanan, Exosomes in bodily fluids are a highly stable resource of disease biomarkers, *Proteomics Clin. Appl.* (2015) 9 358–367.
- [23] K.R. Jakobsen, et al., Exosomal proteins as potential diagnostic markers in advanced non-small cell lung carcinoma, *J. Extracell. Vesicles* 4 (2015) 1–10.
- [24] K. Ueda, et al., Antibody-coupled monolithic silica microtips for highthroughput molecular profiling of circulating exosomes, *Sci. Rep.* 4 (2014) 1–9.
- [25] A.M. Weaver, M. McCabe, I. Kim, M.M. Allietta, S.L. Gonias, Epidermal growth factor and platelet-derived growth factor-BB induce a stable increase in the activity of low density lipoprotein receptor-related protein in vascular smooth muscle cells by altering receptor distribution and recycling, *J. Biol. Chem.* 271 (1996) 24894–24900.
- [26] C. Yoon, et al., Low-density lipoprotein receptor-related protein 1 (LRP1)-dependent cell signaling promotes axonal regeneration, *J. Biol. Chem.* 288 (2013), 26557.
- [27] M. Gorovoy, A. Gaultier, W.M. Campana, G.S. Firestein, S.L. Gonias, Inflammatory mediators promote production of shed LRP1/CD91, which regulates cell signaling and cytokine expression by macrophages, *J. Leukoc. Biol.* 88 (2010) 769–778.
- [28] A. Kinoshita, T. Shah, M.M. Tangredi, D.K. Strickland, B.T. Hyman, The intracellular domain of the low density lipoprotein receptor-related protein modulates transactivation mediated by amyloid precursor protein and Fe65, *J. Biol. Chem.* 278 (2003) 41182–41188.
- [29] S. Pawaria, R.J. Binder, CD91-dependent programming of T helper cell responses following Heat Shock Protein immunization, *Nat. Commun.* 2 (2011) 521.
- [30] K. Egerer, et al., Circulating proteasomes are markers of cell damage and immunologic activity in autoimmune diseases, *J. Rheumatol.* 29 (2002).
- [31] D. Pan, et al., Preferential localization of MUC1 glycoprotein in exosomes secreted by non-small cell lung carcinoma cells, *Int. J. Mol. Sci.* 20 (2019).
- [32] H. Meng, et al., Stromal LRP1 in lung adenocarcinoma predicts clinical outcome, *Clin. Cancer Res.* 17 (2011) 2426–2433.
- [33] C. Lässer, M. Eldh, J. Lötvall, Isolation and characterization of RNA-containing exosomes, *JoVE* (2012) 1–6, <https://doi.org/10.3791/3037>.

- [34] J.M. Escola, et al., Selective enrichment of tetraspan proteins on the internal vesicles of multivesicular endosomes and on exosomes secreted by human B-lymphocytes, *J. Biol. Chem.* 273 (1998) 20121–20127.
- [35] R.A. Haraszti, et al., High-resolution proteomic and lipidomic analysis of exosomes and microvesicles from different cell sources, *J. Extracell. Vesicles* 5 (2016).
- [36] S. Ma, et al., CD63-mediated cloaking of VEGF in small extracellular vesicles contributes to anti-VEGF therapy resistance, *Cell Rep.* 36 (2021).
- [37] K. Ueda, et al., Antibody-coupled monolithic silica microtips for highthroughput molecular profiling of circulating exosomes, *Sci. Rep.* 4 (2014) 1–9.
- [38] P. Boucher, Herz, J. Signaling through LRP1: protection from atherosclerosis and beyond, *Biochem. Pharmacol.* 81 (2011) 1.
- [39] K. Rk, S. Me, H. Mm, Decreased expression of the low density lipoprotein receptor-related protein/alpha 2-macroglobulin receptor in invasive cell clones derived from human prostate and breast tumor cells, *Oncol. Res.* 6 (1994) 365–372.
- [40] T.J. de Vries, et al., Decreased expression of both the low-density lipoprotein receptor-related protein/alpha2-macroglobulin receptor and its receptor-associated protein in late stages of cutaneous melanocytic tumor progression, *Cancer Res.* 56 (1996).
- [41] G. Mb, et al., Decreased expression of the low-density lipoprotein receptor-related protein-1 (LRP-1) in rats with prostate cancer, *J. Histochem. Cytochem.* 51 (2003) 1575–1580.
- [42] H. Xy, et al., Low level of low-density lipoprotein receptor-related protein 1 predicts an unfavorable prognosis of hepatocellular carcinoma after curative resection, *PLoS One* 7 (2012).
- [43] M. V, G. A, L. Rd, C. Wm, G. Sl, The low-density lipoprotein receptor-related protein regulates cancer cell survival and metastasis development, *Cancer Res.* 67 (2007) 9817–9824.
- [44] S. Dedieu, et al., LRP-1 silencing prevents malignant cell invasion despite increased pericellular proteolytic activities, *Mol. Cell Biol.* 28 (2008) 2980.
- [45] B. Chazaud, et al., Promigratory effect of plasminogen activator inhibitor-1 on invasive breast cancer cell populations, *Am. J. Pathol.* 160 (2002) 237.
- [46] L. Catasús, et al., Low-density lipoprotein receptor-related protein 1 (LRP-1) is associated with high-grade, advanced stage and p53 and p16 alterations in endometrial carcinomas, *Histopathology* 59 (2011) 567–571.
- [47] A.L. Sedlacek, et al., CD91 on dendritic cells governs immunosurveillance of nascent, emerging tumors, *JCI Insight* 4 (2019).
- [48] L.B. Kinner-Bibeau, A.L. Sedlacek, M.N. Messmer, S.C. Watkins, R.J. Binder, HSPs drive dichotomous T-cell immune responses via DNA methylome remodelling in antigen presenting cells, 2017 8, *Nat. Commun.* 1 8 (2017) 1–13.
- [49] J. Herz, et al., Surface Location and High Affinity for Calcium of a 500-kd Liver Membrane Protein Closely Related to the LDL-Receptor Suggest a Physiological Role as Lipoprotein Receptor - PubMed, 1988. <https://pubmed.ncbi.nlm.nih.gov/3266596/>.
- [50] D.D. Taylor, W. Zacharias, C. Gercel-Taylor, Exosome isolation for proteomic analyses and RNA profiling, *Methods Mol. Biol.* 728 (2011) 235–246.
- [51] M. Norman, et al., L1CAM is not associated with extracellular vesicles in human cerebrospinal fluid or plasma, 2021, *Nat. Methods* 18 (6 18) (2021) 631–634.